

Rubrosides A–H, New Bioactive Tetramic Acid Glycosides from the Marine Sponge *Siliquariaspongia japonica*¹

Noriko U. Sata,[†] Shun-ichi Wada,[‡] Shigeaki Matsunaga,[†] Shugo Watabe,[‡]
Rob W. M. van Soest,[§] and Nobuhiro Fusetani^{*†}

Laboratory of Aquatic Natural Products Chemistry and Laboratory of Aquatic Molecular Biology and Biotechnology, Graduate School of Agricultural and Life Sciences, The University of Tokyo, Bunkyo-ku, Tokyo 113-8657, Japan, and Institute for Systematics and Ecology, The University of Amsterdam, P.O. Box 94766, 1090 GT Amsterdam, Netherlands

Received October 2, 1998

Eight new tetramic acid glycosides named rubrosides A–H have been isolated from the marine sponge *Siliquariaspongia japonica*. Their structures were elucidated on the basis of spectral data as tetramic acid glycosides containing polyenes terminating in a 4-chloro-2-methyltetrahydrofuran ring. The absolute stereochemistry of the furan functionality in the two major metabolites, rubrosides D and F, was determined by the NMR method using chiral anisotropic reagents for tetrahydro-2-furoic acid derived by RuO₄ oxidation. The absolute stereochemistry of tetramic acid and of the sugar moieties in all rubrosides was deduced by chiral GC analysis of chemical degradation products. The rubrosides induced numerous large intracellular vacuoles in 3Y1 rat fibroblasts at concentrations of 0.5–1.0 μg/mL, and rubrosides A, C, D, and E were cytotoxic against P388 murine leukemia cells with IC₅₀ values of 0.046–0.21 μg/mL. Most rubrosides show antifungal activity against *Aspergillus fumigatus* and *Candida albicans*.

Marine sponges of the order Lithistida have proved to be a rich source of metabolites with unusual structural features as well as interesting biological activities, many of which are reminiscent of microbial metabolites,² e.g., discodermins,³ theonellamides,⁴ swinholides,⁵ discoderimide,⁶ and auranosides.⁷ Faulkner and co-workers showed that swinholides are in fact of bacterial origin.⁸ Recently, we have initiated a program to discover marine natural products that influence cell functions using 3Y1 rat fibroblast cells,⁹ which proved to be useful for detection

of active compounds such as inhibitors of actin polymerization, spindle toxins, cell cycle arrestants, and others. In the screening of a number of extracts, we encountered a vermilion sponge, *Siliquariaspongia japonica*, collected off Hachijo-jima Island, whose methanolic extract exhibited significant activity in the 3Y1 rat fibroblast assay. Bioassay-guided isolation afforded eight active metabolites named rubrosides A–H, which proved to be new tetramic acid glycosides containing an unusual 4-chloro-2-methyl-tetrahydrofuran ring. This paper describes the isolation, structure elucidation, and bioactivities of these compounds.

The EtOH extract of the sponge (400 g wet weight) was partitioned between ether and water. The aqueous phase was extracted with *n*-BuOH, and the ether phase¹⁰ was partitioned between MeOH/H₂O (9:1) and *n*-hexane. The *n*-BuOH and the aqueous MeOH phases were combined and subjected to flash chromatography on ODS followed by reversed-phase HPLC to give rubrosides A (**1**, 9.1 mg, 2.3 × 10⁻³ %), B (**2**, 5.1 mg, 1.3 × 10⁻³ %), C (**3**, 7.0 mg, 1.8 × 10⁻³ %), D (**4**, 126.3 mg, 3.2 × 10⁻² %), E (**5**, 8.6 mg, 2.2 × 10⁻³ %), F (**6**, 108.1 mg, 2.7 × 10⁻² %), G (**7**, 5.5 mg, 1.4 × 10⁻³ %), and H (**8**, 4.5 mg, 1.1 × 10⁻³ %) as dark red solids (Chart 1).

The most abundant rubroside D (**4**) exhibited UV absorptions at 251 and 432 nm in MeOH, which were shifted to 359 and 480 nm in 0.01 N HCl and to 251, 432, and 453 nm in 0.01 N NaOH, reminiscent of the auranosides.⁷ The FABMS revealed (M – H)⁻ ions of equal intensity at *m/z* 939 and 941, indicative of the presence

* To whom correspondence should be addressed. Phone: +81-3-3812-2111 (ext 5299). Fax: +81-3-5684-0622. E-mail: anobu@hongo.ecc.u-tokyo.ac.jp.

[†] Laboratory of Aquatic Natural Products Chemistry.

[‡] Laboratory of Aquatic Molecular Biology and Biotechnology.

[§] Institute for Systematics and Ecology.

(1) Bioactive Marine Metabolites. Part 87. Part 86: Nakao, Y.; Masuda, A.; Matsunaga, S.; Fusetani, N. *J. Am. Chem. Soc.*, in press. (2) Bewley, C. A.; Faulkner, D. J. *Angew. Chem. Int. Ed.* **1998**, *37*, 2162–2178.

(3) (a) Matsunaga, S.; Fusetani, N.; Konosu, S. *Tetrahedron Lett.* **1984**, *25*, 5165–5168. (b) Matsunaga, S.; Fusetani, N.; Konosu, S. *Tetrahedron Lett.* **1985**, *26*, 855–856. (c) Matsunaga, S.; Fusetani, N.; Konosu, S. *J. Nat. Prod.* **1985**, *48*, 236–241. (d) Ryu, G.; Matsunaga, S.; Fusetani, N. *Tetrahedron Lett.* **1994**, *35*, 8251–8254. (e) Ryu, G.; Matsunaga, S.; Fusetani, N. *Tetrahedron* **1994**, *50*, 13409–13416.

(4) (a) Matsunaga, S.; Fusetani, N.; Hashimoto, K.; Walchli, M. *J. Am. Chem. Soc.* **1989**, *111*, 2582–2588. (b) Matsunaga, S.; Fusetani, N. *J. Org. Chem.* **1995**, *60*, 1177–1181.

(5) (a) Carmely, S.; Kashman, Y. *Tetrahedron Lett.* **1985**, *26*, 511–514. (b) Kobayashi, M.; Tanaka, J.; Katori, T.; Matsuura, M.; Kitagawa, I. *Tetrahedron Lett.* **1989**, *30*, 2963–2966. (c) Kobayashi, M.; Tanaka, J.; Katori, T.; Kitagawa, I. *Chem. Pharm. Bull.* **1990**, *38*, 2960–2966. (d) Tsukamoto, S.; Ishibashi, M.; Sasaki, T.; Kobayashi, J. *J. Chem. Soc., Perkin Trans. 1* **1991**, 3185–3188. (e) Tsukamoto, S.; Ishibashi, M.; Sasaki, T.; Kobayashi, J. *J. Chem. Soc., Perkin Trans. 1* **1993**, 1273. (f) Dumdei, E. J.; Blunt, J. W.; Munro, M. H. G.; Pannell, L. K. *J. Org. Chem.* **1997**, *62*, 2636–2639.

(6) Gunasekera, S. P.; Gunasekera, M.; McCarthy, P. *J. Org. Chem.* **1991**, *56*, 4830–4833.

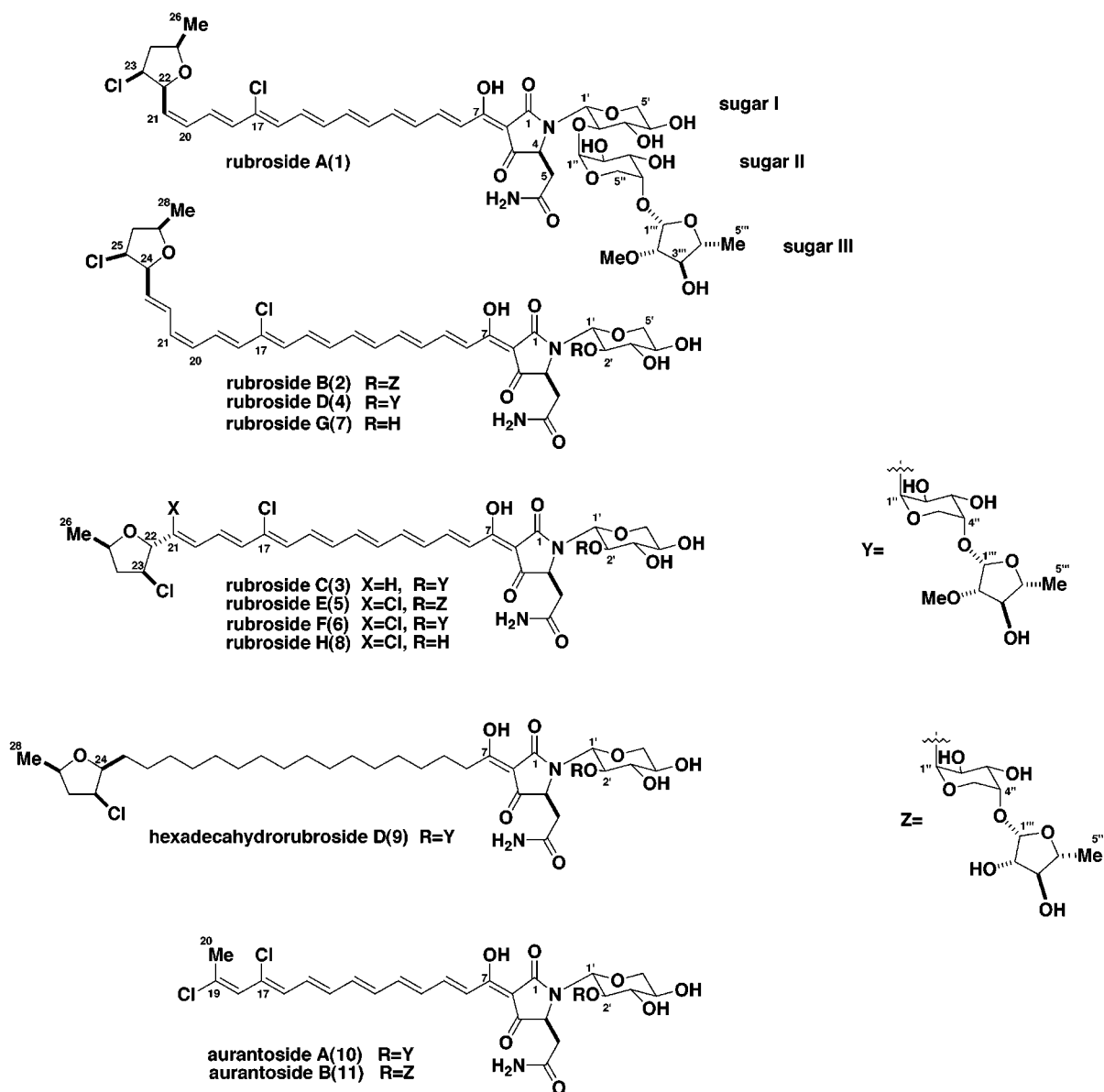
(7) (a) Matsunaga, S.; Fusetani, N.; Kato, Y. *J. Am. Chem. Soc.* **1991**, *113*, 9690–9692. (b) Schmidt, E. W.; Harper, M. K.; Faulkner, D. J. *J. Nat. Prod.* **1997**, *60*, 779–782. The structures of auranosides have been revised as shown (manuscript submitted).

(8) Bewley, C. A.; Holland, N. D.; Faulkner, D. J. *Experientia* **1996**, *52*, 716–722.

(9) (a) Kimura, G.; Itagaki, A.; Summers, J. *Int. J. Cancer* **1975**, *15*, 694–706. (b) Watabe, S.; Wada, S.; Saito, S.; Matsunaga, S.; Fusetani, N.; Ozaki, H.; Karaki, H. *Cell Struct. Funct.* **1996**, *21*, 199–212.

(10) The organic phase was subjected to a series of solvent partitioning between *n*-hexane/MeOH–H₂O (9:1) and CH₂Cl₂/MeOH–H₂O (6:4). The CH₂Cl₂ and 60% aqueous MeOH phases exhibited the activity to induce morphological changes in cultured 3Y1 rat fibroblasts.

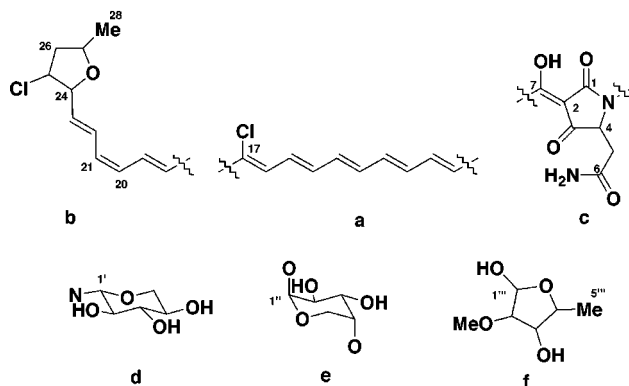
Chart 1



of either one bromine or two or three chlorine atoms. In fact, the molecular formula of $C_{44}H_{56}Cl_2N_2O_{16}$ was determined by HRFABMS. We faced a problem with acquiring NMR data of high quality. Although 1H NMR signals were well dispersed in CD_3OD , they were uniformly broad. Measurement in $DMSO-d_6$ did not solve this problem, which was finally overcome by using pyridine- d_5 as a solvent. Because of slow formation of the pyridinium salt, the 1H NMR spectrum experienced a transition state, appearing as a mixture of two compounds and finally converging to a spectrum of a single compound.¹¹ To determine coupling constants, it was absolutely necessary to measure the 1H NMR spectrum in pyridine- d_5 .

Interpretation of the COSY spectrum starting from a deshielded olefinic signal at δ 7.76 (d, J = 15.0 Hz, H8), together with analysis of coupling constants, led to partial structure **a**, in which all double bonds except for Δ^{16} had

E geometry (Table 1). Similarly, COSY analysis starting



from a doublet at δ 6.52 (d, J = 14.3 Hz, H18) resulted in partial structure **b**, which consisted of a triene connected to a disubstituted tetrahydrofuran ring. Coupling constants indicated *Z* geometry of the Δ^{20} double bond and *E* geometry for other two. Placement of a chlorine atom at C-25 was consistent with 1H and ^{13}C chemical

(11) At higher temperatures, 1H NMR signals became sharper and dispersed. It is interesting that signals of tetramic acid and xylose moieties changed over 4 d at 318 K. Similar results were also observed for other rubrosides.

Table 1. NMR Data for Rubroside D (4) in CD₃OD and C₅D₅N

	CD ₃ OD			C ₅ D ₅ N			HMBC (C no.)
	¹³ C mult	¹ H mult	<i>J</i> (Hz)	¹³ C mult	¹ H mult	<i>J</i> (Hz)	
1	174.8 s			174.0 s			
2	102.5 s			101.7 s			
3	195.0 s			196.1 s			
4	65.4 d	4.32 br		60.3 d	5.32 dd	3.4, 6.7	6, 3
5 α	38.2 t	2.65 m		39.0 t	3.22 dd	6.7, 15.9	4, 6
5 β		2.80 dd	4.9, 12.2		3.37 dd	3.4, 15.9	4, 6, 3
6	174.3 s			172.9 s			
7	176.2 s			174.2 s			
8	122.0 d	7.20 d	14.0	123.6 d	7.76 d	15.0	7, 10
9	146.4 d	7.62 dd	12.2, 14.0	143.7 d	7.64 dd	11.3, 15.0	7, 8, 10, 11
10	133.3 d	6.60 m		133.0 d	6.42 dd	15.0, 11.3	8
11	145.3 d	6.88 m		142.5 d	6.71 dd	11.6, 15.0	9, 13, 12
12	135.6 d	6.58 m		135.2 d	6.46 dd	13.7, 11.6	11, 14
13	140.4 d	6.73 dd	11.3, 15.0	136.8 d	6.57 dd	10.9, 13.7	
14	137.4 d	6.60 m		138.4 d	6.61 dd	13.7, 10.9	
15	132.9 d	6.88 m		131.7 d	6.95 dd	11.0, 13.7	17, 14
16	131.1 d	6.58 m		130.5 d	6.59 d	11.0	17
17	134.9 s			133.8 s			
18	132.7 d	6.53 d	14.0	132.0 d	6.52 d	14.3	17, 20
19	128.8 d	7.17 dd	10.7, 14.0	128.1 d	7.37 dd	11.0, 14.3	20, 21, 17
20	132.1 d	6.20 m		129.8 d	6.22 dd	10.7, 11.0	22, 21
21	130.6 d	6.18 m		131.7 d	6.27 dd	10.7, 10.7	19
22	129.5 d	6.88 m		128.6 d	7.14 dd	15.3, 10.7	24, 20, 21
23	133.1 d	5.92 dd	6.1, 15.0	133.3 d	6.17 dd	6.4, 15.3	25, 24, 21
24	84.1 d	4.50 m		83.0 d	4.49 dd	4.0, 6.4	25
25	63.3 d	4.51 m		63.1 d	4.56 ddd	3.0, 4.0, 6.7	27
26 α	44.9 t	1.92 dd	6.4, 13.6	44.3 t	1.91 ddd	6.7, 7.6, 14.0	25, 27, 24
26 β		2.78 dd	7.3, 13.6		2.62 ddd	3.0, 6.4, 14.0	27, 24
27	75.6 d	4.14 m		74.4 d	4.05 ddd	6.1, 6.4, 7.6	
28	22.2 q	1.38 d	6.1	22.1 q	1.36 d	6.1	27, 26
NH ₂					7.80 brs 8.40 brs		
1'	86.1 d			80.9 d	6.10 d	9.2	4, 5', 2', 1
2'	81.3 d	4.50 br		81.6 d	4.68 dd	8.9, 9.2	1', 1''
3'	79.2 d	3.47 t	8.9	69.9 d	4.18 m		2', 5'
4'	70.5 d	3.61 m		79.7 d	4.24 m		
5' α	69.2 t	3.21 t	11.0	69.4 t	3.64 t	12.0	3', 4', 1'
5' β		3.86 m			4.24 m		
1''	103.9 d	5.02 brs		104.2 d	5.75 d	3.4	5'', 3'', 2'
2''	71.6 d	3.79 m		71.5 d	4.43 dd	5.0, 9.8	3''
3''	70.8 d	3.78 m		70.1 d	4.38 dd	3.1, 9.8	2'', 4''
4''	76.0 d	3.91 m		76.9 d	4.20 m		1'', 2''
5'' α	61.5 t	3.57 m		61.8 t	4.02 m		1'', 4'', 3''
5'' β		3.70 m			4.24 m		4''
1'''	98.9 d	5.08 d	4.3	99.7 d	5.29 d	4.5	4'', 3'''
2'''	87.3 d	3.64 m		87.2 d	3.91 dd	4.5, 7.8	OMe, 3'''
3'''	79.7 d	3.89 m		79.1 d	4.41 t	7.8	2''', 4'''
4'''	79.5 d	3.74 m		79.1 d	4.12 t	6.4	3''', 1'''
5'''	20.8 q	1.31 d	6.1	20.9 d	1.44 d	6.4	4'''
OMe	58.3 q	3.34 s		57.6 q	3.35 s		2'''

shifts of δ 4.56 and 63.1, respectively. The presence of a tetrahydrofuran ring was implied by a NOESY cross-peak between H-24 and H-27 and supported by coupling constants for H-24 to H-27, which were observed between 3.0 and 7.6 Hz.¹² Units **a** and **b** were connected through C-17/C-18 on the basis of the HMBC cross-peaks, H-18/C-17 and H-16/C-17 (Table 1). We were not able to use NOESY or ROESY data to assign stereochemistry of the Δ^{16} -olefin because signals for H-16 and H-18 were overlapped with those for H-13 and H-14, respectively; the four signals were congested in a range of approximately 0.1 ppm. Therefore, *Z* geometry for this olefin was inferred from: (1) chemical shifts of H-13 through H-15 similar to those in aurantiosides, especially the significant downfield shift of H-15 due to the proximate chlorine atom, and (2) the absence of a ROESY cross-peak between H-15 and H-18. Instead, a distinct ROESY cross-peak was observed between H-19 and H-22.

There was a pair of mutually coupled exchangeable broad singlets at δ 7.80 and 8.40 in the ¹H NMR spectrum that exhibited NOESY cross-peaks with the methylene protons in an isolated CHCH₂ unit (C-4, C-5), thereby suggesting the presence of a primary amide, which was confirmed by HMBC data (H-4/C-6, H-5 α /C-6, and H-5 β /C-6). Four broad nonprotonated ¹³C NMR signals at δ 196.1, 174.0, 174.2, and 101.7¹³ were reminiscent of the tetramic acid portion of the aurantiosides, which was also supported by acid/base shifts of UV absorptions and by HMBC cross-peaks H-4, H-5 β , and C-3 at δ 196.1 (unit

(12) Stevens, J. D.; Fetcher, H. G., Jr. *J. Org. Chem.* **1968**, *33*, 1799–1805.

(13) (a) Shigemori, H.; Bae, M.-A.; Yazawa, K.; Sasaki, T.; Kobayashi, J. *J. Org. Chem.* **1992**, *57*, 4317–4320. (b) Kanazawa, S.; Fusetani, N.; Matsunaga, S. *Tetrahedron Lett.* **1993**, *34*, 1065–1068. (c) Ohta, S.; Ohta, E.; Ikegami, S. *J. Org. Chem.* **1997**, *62*, 6452–6453. (d) Lee, V. J.; Rinehart, K. L., Jr. *J. Antibiot.* **1980**, *33*, 408–415. (e) Stickings, C. E. *Biochem. J.* **1959**, *72*, 332–340. (f) Phillips, N. J.; Goodwin, J. T.; Fraiman, A.; Cole, R. J.; Lynn, D. G. *J. Am. Chem. Soc.* **1989**, *111*, 8223–8231. (g) Sakuda, S.; Ono, M.; Furihata, K.; Nakayama, J.; Suzuki, A.; Isogai, A. *J. Am. Chem. Soc.* **1996**, *118*, 7855–7856. (h) Nowak, A.; Steffan, B. *Liebigs Ann. Chem.* **1997**, 1817–1821.

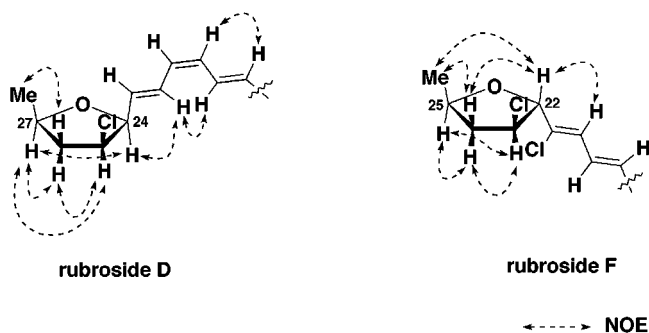


Figure 1. Comparison of NOESY data of rubrosides D and F in C_5D_5N .

c); connectivities of units **b** and **c** could be established by HMBC cross-peaks H-8/C-7 and H-9/C-7 (Table 1).

The remaining portion consisted of three sugars, each of which gave rise to an isolated spin system starting from an anomeric proton. Interpretation of the HOHAHA and COSY spectra together with HMQC data led to assignment of a xylopyranose unit with an axial anomeric proton (sugar I), an arabinopyranose unit with an equatorial anomeric proton (sugar II), and a 5-deoxypentofuranose unit (sugar III) possessing a methoxy group on C-2''' as revealed by HMBC correlations ($OCH_3/C-2'''$ and H-2'''/ OCH_3). The sequence of the three sugars was established by HMBC cross-peaks observed between H-1''' (δ 5.29) and C-4'' (76.9) and H-1'' (5.75) and C-2' (81.6). A chemical shift of δ 80.9 for C-1' and an HMBC cross-peak between H-1' (δ 6.10) and a carbon at δ 174.0, which was a part of tetramic acid, indicated that the xylopyranose unit was linked to the tetramic acid unit through a nitrogen atom. At this stage, we realized that the gross structure of the glycosylated tetramic acid moiety in rubroside D was identical with the corresponding portion in aurantoside A. This was supported by NMR data of the relevant portions, which were almost superimposable on those of aurantoside A (**10**), thus suggesting their identical stereochemistry.

Treatment of **4** with H_2 on Pd-C in MeOH afforded a hexadecahydrorubroside D (**9**) in good yield. The 1H NMR spectrum exhibited a broad signal at δ 1.23 for a long methylene chain from H-8 to H-24, and the FABMS showed a pseudomolecular ion at m/z 919 ($M - H$)⁻, corresponding to $C_{44}H_{72}ClN_2O_{16}$.

Stereochemistry of C-4 was determined as *S* by the same method applied to aurantosides.⁷ Lemieux oxidation¹⁴ followed by acid hydrolysis of rubroside D yielded L-Asp as analyzed by chiral GC analysis. The relative stereochemistry of the terminal tetrahydrofuran ring was established on the basis of NOESY correlations, H-24/H-27, H-25/H-27, H-26 α /H-27, H-25/H-26 α , and CH_3 -28/H-26 β (Figure 1), which disclosed that H-24, H-25, and H-27 were on the same face of the five-membered ring. To determine its absolute stereochemistry, we decided to apply the NMR method using the chiral anisotropic reagents (*R*)- and (*S*)-phenylglycine methyl esters (PGME)¹⁵ developed by Kusumi and co-worker¹⁶ to a furoic acid derived by cleavage of the C-22-C-23 double bond. First, we examined the validity of this method by using (*R*)- and (*S*)-tetrahydro-2-furoic acids as suitable

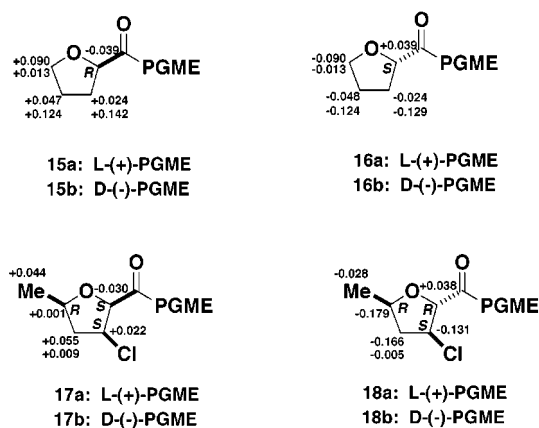


Figure 2. $\Delta\delta$ values obtained for tetrahydro-2-furoic acid and 3-chloro-5-methyl-tetrahydro-2-furoic acid PGME esters. $\Delta\delta = \delta_{S(-)} - \delta_{R(+)}$.

models. Unexpectedly, the $\Delta\delta$ values of the (*R*)-PGME amide were all positive except for the α -H, which gave a negative value, whereas the reverse was true for (*S*)-PGME amide (Figure 2). It is likely that the conformation of the chiral auxiliary was different from the reported model as a result of the formation of a hydrogen bond between the amide hydrogen and the ether oxygen. If the pattern of distribution of $\Delta\delta$ values was reproducible in our system, it should be possible to assign the absolute stereochemistry. Rubroside D (**4**) was oxidized with ruthenium tetroxide¹⁷ to give 3-chloro-5-methyl-tetrahydro-2-furoic acid (**17**), which was converted to the PGME amides **17a** and **17b**. The $\Delta\delta$ values were positive for all the protons except for the α -H (Figure 2). Therefore, the stereochemistry of the methine carbon attached to the carboxylic group was assigned as *S*. Incidentally, the formation of a hydrogen bond between the amide NH and the chlorine atom was ruled out by comparing the $\Delta\delta$ values of the PGME amides.

The absolute stereochemistry of both xylose and arabinose were determined to be *D* by chiral GC analysis of the acid hydrolysate.¹⁸ The relative stereochemistry of sugar III was assigned on the basis of NOESY correlations H-1'''/H-3''', H-1'''/H-4''', and H-3'''/CH₃-5''' to be identical with 5-deoxyarabinoside in aurantoside A, which was supported by almost superimposable 1H and ^{13}C NMR values for the relevant portions. Because attempts to determine the absolute stereochemistry by the Mosher method¹⁹ were not successful, we decided to isolate sugar III. Rubroside D was subjected to methanolysis followed by ODS flash chromatography to furnish the methyl glycoside of sugar III. Distribution of the positive and negative $\Delta\delta$ values of the MTPA esters was in agreement with 3''' *R* stereochemistry (Figure 3). It is in agreement with the stereochemistry of des-*O*-methyl sugar III in aurantoside B,⁷ which had been assigned by the CD exciton chirality method.²⁰

Rubroside F (**6**) had a molecular formula of $C_{42}H_{53}Cl_3N_2O_{16}$, which differs from **4** by the elements of C_2H_3 -

(17) Carlsen, P. H.; Katsuki, T.; Martin, V. S.; Sharpless, K. B. *J. Org. Chem.* **1981**, *46*, 3936–3938.

(18) Kinig, W. A.; Benecke, I.; Bretting, H. *Angew. Chem., Int. Ed. Engl.* **1981**, *20*, 693–694.

(19) Ohtani, I.; Kusumi, T.; Kashman, Y.; Kakisawa, H. *J. Am. Chem. Soc.* **1991**, *113*, 4092–4096.

(20) Nakanishi, K.; Kuroyanagi, M.; Nambu, H.; Oltz, E. M.; Takeda, R.; Verdine, G.; Zask, A. *Pure Appl. Chem.* **1984**, *56*, 1031–1048.

(14) (a) Lemieux, R. U. *Anal. Chem.* **1954**, *26*, 920–921. (b) Lemieux, R. U.; Johnson, W. S. *J. Org. Chem.* **1956**, *21*, 478–479.

(15) Rachele, J. R. *J. Org. Chem.* **1963**, *28*, 2898.

(16) Nagai, Y.; Kusumi, T. *Tetrahedron Lett.* **1995**, *36*, 1853–1856.

Table 2. ¹H NMR Data for Rubrosides A (1), B (2), and G (7)

	1 ^a	2 ^b	7 ^a
4	4.31 br	4.20 br	4.29 br
5α	2.66 br	2.52	2.80 m
5β	2.80 m	2.60	
8	7.22 br	7.19 br	7.25 d (15.2)
9	7.61 br	7.55 br	7.63 dd (11.9, 15.2)
10	6.62 m	6.88 m	6.63 m
11	6.90 m	7.04 m	6.73 dd (11.0, 16.0)
12	6.57 m	6.67 m	6.57 m
13	6.70 dd (11.0, 13.8)	6.70 m	6.58 m
14	6.63 m	6.72 m	6.59 m
15	6.88 m	6.80 m	6.90 m
16	6.59 m	6.70 m	6.61 m
17			
18	6.53 d (14.0)	6.69 d (15.0)	6.51 d (14.4)
19	7.00 dd (11.5, 14.0)	7.05 dd (10.1, 15.0)	7.17 dd (10.7, 14.4)
20	6.40 dd (10.4, 11.5)	6.23 m	6.20 dd (11.0, 10.7)
21	5.72 dd (7.6, 10.4)	6.21 m	6.17 dd (10.7, 11.0)
22	4.88 br	6.86 dd (10.4, 15.2)	6.88 m
23	4.54 ddd (2.4, 2.7, 6.4)	5.89 dd (6.6, 15.2)	5.92 dd (6.4, 15.0)
24α	1.94 ddd (2.4, 6.1, 14.3)	4.52 dd (4.0, 6.6)	4.50 m
24β	2.84 ddd (6.4, 8.2, 4.3)		
25	4.15 ddq (6.1, 6.1, 8.2)	4.69 ddd (3.1, 7.0, 4.0)	4.52 m
26α	1.37 d (6.1)	1.84 ddd (3.1, 6.1, 14.3)	1.92 ddd (2.4, 6.1, 14.0)
26β		2.77 ddd (7.0, 7.6, 14.3)	2.77 ddd (6.4, 7.9, 14.0)
27		4.08 m	4.14 dq (6.4, 7.9)
28		1.32 d (6.1)	1.38 d (6.4)
NH ₂		6.99 brs	
		7.44 brs	
1'			4.77 br
2'			4.02 br
3'	3.47 t (8.9)	3.30 m	3.32 m
4'	3.61 m	3.40 m	3.54 ddd (5.5, 9.5, 9.7)
5'α	3.21 dd (7.6, 14.4)	3.10 t (10.7)	3.23 dd (9.7, 11.2)
5'β	3.87 m	3.73 m	3.87 dd (5.5, 11.2)
1''	5.02 br	4.83 brs	
2''	3.78 m	3.61 m	
3''	3.78 m	3.60 m	
4''	3.90 m	3.80 m	
5''α	3.57 dd (2.7, 12.5)	3.41 m	
5''β	3.70	3.53 m	
1'''	5.08 d (4.0)	4.81 d (4.6)	
2'''	3.67 m	3.71 m	
3'''	3.87 m	3.61 m	
4'''	3.75 m	3.61 m	
5'''	1.31 d (6.1)	1.21 d (5.8)	
OMe	3.34 s		

^a CD₃OD at 300 K. ^b DMSO-*d*₆ at 300 K.

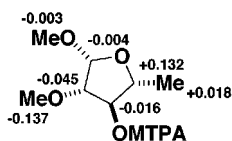


Figure 3. $\Delta\delta$ values obtained for 5-deoxy-1,2-dimethoxy-arabinose MTPA ester. $\Delta\delta = \delta_{S(-)} - \delta_{R(+)}$.

Cl. One double bond was missing, and an additional chlorine atom was present. NMR data suggested that **6** duplicated partial structures including relative stereochemistry of the tetramic acid, sugar, and polyene portions up to C-17 of **4** (Tables 3 and 4). Six contiguous olefinic protons (H-18 through H-23) in **4** were replaced by three mutually coupled olefinic signals. The COSY spectrum revealed the proton signals attributable to the terminal tetrahydrofuran ring, but their chemical shifts and coupling constants were significantly different from those in **4**. HMBC data indicated that C-17 and the tetrahydrofuran ring were connected via a 1-chlorobutadiene unit; a nonprotonated carbon (C-21) at δ 134.3 was linked to a methine proton at δ 4.81 (H-22) on the tetrahydrofuran ring.

Chiral GC analysis of the methanolysis products revealed D configuration for both xylose and arabinose, and analysis of the Lemieux oxidation/acid hydrolysis product implied 4*S* stereochemistry for the tetramic acid portion. The relative stereochemistry of the terminal tetrahydrofuran ring was assigned on the basis of NOESY cross-peaks H-22/H-24 β , H-22/CH₃-26, H-23/H-24 α , H-23/H-25, H-24 α /H-25, and H-24 β /CH₃-26 (Figure 1), which indicated that H-23 and H-25 were on the same face of the tetrahydrofuran ring and H-22 and CH₃-26 were on the opposite face. Absolute stereochemistry at C-22 was determined in the same manner as in the case of **4**. Oxidation of **6** with RuO₄ yielded **18**, which was converted to the PGME amides **18a** and **18b**. The $\Delta\delta$ values were negative for all of the protons except for the α -hydrogen (Figure 2), thus revealing that the tetrahydrofuran ring in **6** was epimeric to that of **4** at the carbon attached to the polyene chain.

Rubroside A (**1**) was smaller by a C₂H₂ unit than rubroside D (**4**). Comparison of COSY, HMQC, and HMBC data showed that they had the identical structure except that the Δ^{22} -olefin in **4** was missing in **1**. *Z* geometry for the Δ^{20} -olefin was deduced from a coupling

Table 3. ^1H NMR Data for Rubrosides **C** (**3**), **E** (**5**), **F** (**6**), and **H** (**8**)

	3 ^a	5 ^b	6 ^c	8 ^d
4	4.31 br	5.48 br	5.35 dd (2.7, 6.5)	4.78 br
5 α	2.64 m	3.30 br	3.24 dd (6.5, 15.6)	3.16 br
5 β	2.79 dd (4.0, 15.9)	3.44 dd (3.5, 16.5)	3.41 dd (2.7, 15.6)	3.45 brd (11.9)
8	7.21 d (15.0)	7.89 br	7.89 d (15.3) ^e	8.12
9	7.61 dd (11.3, 15.0)	7.60 br	7.65 dd (11.3, 15.3) ^e	7.65 dd (11.9, 14.2)
10	6.62 m	6.45 m	6.41 dd (14.7, 11.3) ^e	6.43 m
11	6.90 m	6.66 m	6.68 dd (11.3, 14.7) ^e	6.61 m
12	6.55 m	6.46 m	6.47 dd (13.8, 11.3) ^e	6.43 m
13	6.72 m	6.56 m	6.59 dd (9.2, 13.8) ^e	6.54 m
14	6.61 m	6.56 m	6.59 dd (13.8, 9.2) ^e	6.54 m
15	6.88 m	6.91 m	6.91 dd (11.1, 13.8) ^e	6.86 m
16	6.57 d (11.3)	6.67 d (11.2)	6.67 d (11.1) ^e	6.63 d (11.2)
17				
18	6.50 d (14.6)	6.70 d (15.0)	6.70 d (14.7) ^e	6.68 d (15.0)
19	6.70 m	7.18 dd (10.8, 15.0)	7.17 dd (10.9, 14.7) ^e	7.16 dd (11.0, 15.0)
20	6.48 dd (10.7, 15.3)	6.83 d (10.8)	6.83 d (10.9) ^e	6.80 d (11.0)
21	5.86 dd (6.7, 15.3)			
22	4.42 t (6.4)	4.82 d (6.2)	4.81 d (5.9)	4.82 d (5.8)
23	4.12 q (7.0)	4.58 ddd (6.2, 6.9, 7.3)	4.57 ddd (5.9, 6.4, 8.3)	4.57 ddd (6.9, 7.3, 5.8)
24 α	1.82 ddd (7.6, 7.9, 12.8)	1.86 ddd (7.3, 8.1, 12.7)	1.85 ddd (8.3, 8.3, 12.7)	1.86 ddd (7.3, 8.1, 12.7)
24 β	2.68 m	2.57 ddd (6.2, 6.9, 12.7)	2.56 ddd (6.4, 6.4, 12.7)	2.57 ddd (6.9, 6.5, 12.7)
25	4.27 m	4.30 m	4.30 ddq (6.3, 6.4, 8.3)	4.31 m
26	1.26 d (6.4)	1.26 d (6.2)	1.25 d (6.3)	1.27 d (6.2)
27				
28				
NH ₂		7.60 brs	7.75 brs	7.56 brs
		7.89 brs	8.31 brs	7.87 brs
1'			6.13 d (8.3)	5.92
2'	3.74 m		4.72 br	4.55
3'	3.46 t (9.2)	4.30 m	4.17 m	4.17 t (9.2)
4'	3.61 m	4.15 m	4.22 m	4.21 m
5' α	3.21 t (11.0)	3.75 dd (10.4, 11.6)	3.63 t (10.3)	3.77 t (10.4)
5' β	3.87 m	4.29 m	4.22 m	4.30 m
1''	5.02 brd (2.8)	5.76 br	5.79 d (3.9)	
2''	3.77 m	4.41 m	4.44 dd (3.9, 10.0)	
3''	3.77 m	4.41 m	4.38 dd (3.4, 10.0)	
4''	3.91 m	4.22 m	4.18 m	
5'' α	3.56 dd (2.7, 12.5)	3.98 brd (11.5)	4.05 dd (2.4, 12.7)	
5'' β	3.68	4.23 m	4.24 m	
1'''	5.08 d (4.6)	5.28 d (4.6)	5.27 d (4.4)	
2'''	3.64 m	4.47 m	3.91 dd (4.4, 7.8)	
3'''	3.89 m	4.43 m	4.41 m	
4'''	3.72 m	4.18 t (6.5)	4.12 dd (6.4, 6.8)	
5'''	1.28 d (5.5)	1.49 d (6.5)	1.44 d (6.4)	
OMe	3.33 s		3.32 s	

^a CD₃OD at 300 K. ^b C₅D₅N at 300 K. ^c C₅D₅N at 313 K. ^d C₅D₅N at 308 K. ^e Coupling constants were determined at 333 K.

constant of 10.4 Hz, whereas the geometry of other olefins was assigned as *E*. Relative stereochemistry of the terminal tetrahydrofuran ring was identical with that of **4** by comparison of the NMR data of the relevant protons.

The HRFAB mass spectrum of rubroside **B** (**2**) led to the molecular formula of C₄₃H₅₄Cl₂N₂O₁₆, which was one CH₂ unit smaller than that of **4**. Absence of an *O*-methyl signal in the ^1H and ^{13}C NMR spectra and an upfield shift of C-2''' (δ 77.5) were consistent with the replacement of the 2''' OMe group in **4** by a hydroxyl group.

Rubroside **C** (**3**) had the same molecular formula as rubroside **A** (**1**). They were different in the terminal portion; **3** had a tetrahydrofuran ring identical with that of **6** and (*E*)- Δ^{20} -olefin was assigned by a coupling constant of 15.3 Hz. The rest of the molecule was identical, as revealed by NMR data.

Rubroside **E** (**5**) was smaller by a CH₂ unit than rubroside **F** (**6**). Their NMR data were superimposable except for the absence of the *O*-methyl signal and an upfield shift of C-2''' in **5**, thereby demonstrating that rubroside **E** is the 2'''-des-*O*-methyl derivative of rubroside **F**.

Rubroside **G** (**7**) had a molecular formula of C₃₃H₃₈-Cl₂N₂O₉, which was significantly smaller than those of the other congeners. It exhibited a ^1H NMR spectrum less crowded in the region between δ 3.00 and 5.00, whereas signals in other regions were superimposable on those of rubroside **D**. Interpretation of 2D NMR data revealed the presence of a xylose moiety with an axial anomeric proton and the absence of the other two sugars. Therefore, rubroside **G** is a truncated derivative of rubroside **D**.

Rubroside **H** (**8**) showed features similar to those of rubroside **G**; the two terminal sugars were missing, and the remainder was superimposable on that of rubroside **F** (**6**). Thus, **8** is a truncated derivative of rubroside **F**.

The rubrosides not only induced morphological changes in 3Y1 rat fibroblasts but also were cytotoxic against P388 murine leukemia cells and antifungal as depicted in Table 5. Rubrosides induced numerous large vacuoles and/or spindle-shaped cells in 3Y1 rat fibroblasts, which may have resulted from disruption of membrane trafficking and/or reduction of the adhesive ability of cells. Interestingly, hexadecahydro-rubroside **D** (**9**) was inactive

Table 4. ^{13}C NMR Data for Rubrosides A (1), B (2), C (3), E (5), F (6), G (7), and H (8)

	1 ^a	2 ^b	3 ^a	5 ^c	6 ^a	7 ^c	8 ^d
1					173.8 s	176.5 s	
2					102.1 s		
3					195.6 s	195.0 s	
4				60.0 d	59.7 d	59.8 d	59.5 d
5	38.2 t	36.5 t	38.0 t	39.0 t	38.8 t	38.5 t	39.0 t
6		170.5 s			172.4 s	173.0 s	
7					174.8 s		
8	122.2 d	120.6 d	121.8 d		124.2 d		
9	146.3 d	144.1 d	146.6 d	142.7 d	142.5 d	140.5 d	141.1 d
10	133.4 d	132.5 d	134.2 d	133.8 d	132.6 d	134.8 d	134.0 d
11	145.1 d	143.7 d	145.2 d	141.6 d	141.4 d	140.0 d	140.2 d
12	135.7 d	134.9 d	135.5 d	135.6 d	134.1 d	134.1 d	135.8 d
13	140.2 d	138.7 d	140.2 d	137.8 d	137.4 d	137.0 d	136.8 d
14	137.7 d	136.8 d	137.3 d	137.8 d	137.4 d	136.8 d	137.7 d
15	132.7 d	130.3 d	132.1 d	130.9 d	130.7 d	130.6 d	130.2 d
16	131.5 d	131.1 d	131.0 d	132.0 d	131.7 d	130.4 d	131.8 d
17	134.5 s	132.6 s			133.2 s	133.0 s	133.5 s
18	134.0 d	131.5 d	132.6 d	134.3 d	133.2 d	132.0 d	134.4 d
19	128.7 d	127.1 d	132.5 d	126.4 d	126.0 d	127.9 d	126.0 d
20	132.5 d	129.0 d	134.2 d	127.4 d	127.0 d	130.0 d	127.2 d
21	130.6 d	131.1 d	134.2 d		134.3 s	131.5 d	134.5 s
22	79.7 d	127.8 d	87.0 d	89.0 d	88.4 d	128.6 d	89.0 d
23	63.5 d	132.9 d	61.5 d	59.5 d	58.9 d	133.2 d	59.3 d
24	45.1 t	82.3 d	44.5 t	43.5 t	43.2 t	83.0 d	43.0 t
25	75.7 d	63.0 d	75.5 d	76.5 d	74.0 d	63.0 d	76.0 d
26	22.2 q	43.5 t	22.0 q	22.0 q	21.2 q	44.2 t	22.0 q
27		73.5 d				74.3 d	
28		22.0 q				22.3 q	
NH ₂							
1'					80.3 d	84.9 d	84.6 d
2'	81.3 d	85.9 d	81.0 d		81.2 d	71.8 d	71.9 d
3'	79.3 d	77.0 d	79.0 d	70.0 d	79.3 d	79.7 d	79.5 d
4'	70.5 d	69.0 d	70.1 d	79.4 d	69.8 d	71.0 d	70.9 d
5'	69.2 t	67.5 t	69.0 t	69.4 t	69.0 t	69.6 t	69.5 t
1''	103.8 d	102.0 d	104.0 d	104.5 d	103.5 d		
2''	71.6 d	69.8 d	71.5 d	70.8 d	71.0 d		
3''	70.8 d	68.5 d	70.3 d	70.2 d	69.4 d		
4''	76.0 d	73.5 d	76.0 d	76.2 d	76.3 d		
5''	61.5 t	60.0 t	61.5 t	61.2 d	61.2 t		
1'''	98.9 d	98.0 d	98.5 d	102.0 d	99.0 d		
2'''	87.3 d	77.5 d	87.0 d	77.8 d	86.7 d		
3'''	79.7 d	77.8 d	79.8 d	74.9 d	78.7 d		
4'''	79.5 d	79.7 d	79.5 d	79.0 d	78.7 d		
5'''	20.8 q	20.5 q	20.5 q	21.5 d	20.6 q		
OMe	58.3 q		58.0 q		57.1 q		

^a CD₃OD at 300 K. ^b DMSO-*d*₆ at 300 K. ^c C₅D₅N at 300 K. ^d C₅D₅N at 308 K.

in all tests, and aurantosides A (10) and B (11) were less active in 3Y1 rat fibroblast and cytotoxic tests. Rubrosides are closely related to aurantosides in having the common tetramic acid core with a C₂ side chain. The appending trisaccharide moiety and the polyene up to C-17 were also identical. Aurantosides terminate in olefins, whereas rubrosides terminate in a tetrahydrofuran ring. The presence of a terminal tetrahydrofuran ring at the end of a polyene conjugated with tetramic acid is reminiscent of erythrokyrin and lipomycin, which were isolated from *Penicillium islandicum*²¹ and *Streptomyces aureofaciens*,²² respectively. Another interesting structural feature of the rubrosides is the presence of Z-olefins in the polyene unit.

Experimental Section

General Experimental Procedures. The NMR spectra were recorded on either a JEOL α -500 or α -600 spectrometer. Chemical shifts were referenced to the solvent (δ_{C} 49.0, δ_{H} 3.30

in CD₃OD; δ_{C} 39.5, δ_{H} 2.49 in DMSO-*d*₆; δ_{C} 123.5, δ_{H} 7.19 in C₅D₅N). Standard pulse sequences were employed for the 2D NMR experiments.²³ NOESY spectra were measured with a mixing time (tm) of 500 ms. FAB mass spectra were obtained on a JEOL SX102 spectrometer. Optical rotations were measured on a JASCO DIP-371 digital polarimeter. IR spectra were recorded on a JASCO FT/IR-5300 Fourier transform infrared spectrometer.

Collection, Extraction, and Isolation. The vermilion sponge *S. japonica* (family Theonellidae, order Lithistida) was collected at a depth of 15 m off Hachijo-jima Island, 300 km south of Tokyo. The main skeleton was an interlocked mass of small tetracrepid desmas of 150 μm diameter which were caltrop-like in having the cladi more or less equal in length and shape. These desmas have characteristic conical spines. At the surface, there was a thin discontinuous layer of discotriaenes with diameter 100–140 μm , with rounded or slightly irregular outline and irregular margins, that had very short rhabds. Microrhabds formed a thick cover at the surface and were dispersed in the interior. They were of three sorts: small thin centrotolote, ca. 18 μm \times 0.5 μm ; long profusely spined oxeotes, ca. 35 μm \times 4 μm ; and thick, almost smooth spindles, ca. 25 μm \times 6 μm . A voucher specimen (ZMAPOR. 13013) was deposited at the Zoological Museum of the University of Amsterdam, The Netherlands. The frozen sponge (400 g wet wt) was sequentially extracted with EtOH (3 \times 1 L). The EtOH extract was concentrated and partitioned between H₂O (500 mL) and Et₂O (3 \times 500 mL). The Et₂O phase was partitioned between *n*-hexane and MeOH/H₂O (9:1). The latter phase was partitioned between H₂O and *n*-BuOH. The active *n*-BuOH and 90% MeOH soluble portions were combined to yield a residue (2.5 g), which was flash chromatographed on ODS with aqueous MeOH. The 90% MeOH eluate was fractionated by MPLC on ODS with CH₃CN/H₂O (55:45) containing 0.05% TFA to yield nine fractions. The second fraction was separated by C₁₈ reversed-phase HPLC with CH₃CN/H₂O (55:45) containing 0.05% TFA, followed by MeOH/H₂O (85:15) containing 0.05% TFA to afford rubroside A (1, 9.1 mg, 2.3 \times 10⁻³), rubroside B (2, 5.1 mg, 1.3 \times 10⁻³), and rubroside C (3, 7.0 mg, 1.8 \times 10⁻³). The third fraction was purified by C₁₈ reversed-phase HPLC with CH₃CN/H₂O (55:45) containing 0.05% TFA, followed by MeOH/H₂O (85:15) containing 0.05% TFA to furnish rubroside D (4, 126.3 mg, 3.2 \times 10⁻²) and rubroside E (5, 8.6 mg, 2.2 \times 10⁻³). The fourth fraction was purified by C₁₈ reversed-phase HPLC with CH₃CN/H₂O (55:45) containing 0.05% TFA and then with MeOH/H₂O (90:10) containing 0.05% TFA to afford rubroside F (6, 108.1 mg, 2.7 \times 10⁻²). The fifth fraction was purified with C₁₈ reversed-phase HPLC with CH₃CN/H₂O (55:45) containing 0.05% TFA, followed by MeOH/H₂O (90:10) containing 0.05% TFA and then CH₃CN/H₂O (60:40) containing 0.05% TFA to yield rubroside G (7, 5.5 mg, 1.4 \times 10⁻³). The sixth fraction was purified with CH₃CN/H₂O (55:45) containing 0.05% TFA, followed by MeOH/H₂O (90:10) containing 0.05% TFA to obtain rubroside H (8, 4.5 mg, 1.1 \times 10⁻³ % wet weight).

Rubroside A (1). Red amorphous solid. $[\alpha]_{\text{D}}^{24}$ -1824° (*c* 0.001, MeOH); UV (MeOH) λ_{max} 246 (ϵ 29 100), 418 (110 400), 430 (110 200) nm; HRFABMS (matrix: glycerol) *m/z* 912.2859 (M - H)⁻ (C₄₂H₅₄³⁵Cl₂N₂O₁₆ Δ +0.9 mmu); ¹H and ¹³C NMR data, see Tables 2 and 4.

Rubroside B (2). Red amorphous solid. $[\alpha]_{\text{D}}^{24}$ -1460° (*c* 0.001, MeOH); UV (MeOH) λ_{max} 250 (ϵ 18 900), 432 (71 300), 457 (69 700) nm; HRFABMS (matrix: glycerol) *m/z* 924.2806 (M - H)⁻ (C₄₃H₅₄³⁵Cl₂N₂O₁₆ Δ -4.5 mmu); ¹H and ¹³C NMR data, see Tables 2 and 4.

Rubroside C (3). Red amorphous solid. $[\alpha]_{\text{D}}^{24}$ -1088° (*c* 0.001, MeOH); UV (MeOH) λ_{max} 240 (ϵ 18 600), 450 (60 600) nm; HRFABMS (matrix: glycerol) *m/z* 912.2794 (M - H)⁻ (C₄₂H₅₄³⁵Cl₂N₂O₁₆ Δ -5.7 mmu); ¹H and ¹³C NMR data, see Tables 3 and 4.

(21) Beutler, J. A.; Hilton, B. D.; Clark, P. *J. Nat. Prod.* **1988**, *51*, 562–566.

(22) Schabacher, K.; Zeeck, A. *Tetrahedron Lett.* **1973**, 2691–2694.

(23) (a) Summers, M. F.; Marzilli, L. G.; Bax, A. *J. Am. Chem. Soc.* **1986**, *108*, 4285–4294. (b) Bax, A.; Subramanians, S. *J. Magn. Reson.* **1986**, *67*, 565–569. (c) Bax, A.; Azolos, A.; Dinya, Z.; Sudo, K. *J. Am. Chem. Soc.* **1986**, *108*, 8056–8063.

Table 5. Biological Activities of Rubrosides

	morphological change in 3Y1 cells ^a	cytotoxicity		antifungal activity ^b	
		P388 cells (IC ₅₀ μg/mL)		<i>C. albicans</i>	<i>A. fumigatus</i>
rubroside A (1)	vacuole,spindles	0.05		11.2	17.8
rubroside B (2)	vacuole	>0.5		inactive	9.5
rubroside C (3)	vacuole,spindles	0.2		inactive	11.0
rubroside D (4)	vacuole	0.2		inactive	10.6
rubroside E (5)	vacuole,spindles	0.2		inactive	inactive
rubroside F (6)	vacuole	0.2		inactive	10.0
rubroside G (7)	vacuole	>0.5		inactive	inactive
rubroside H (8)	no change	>0.5		inactive	inactive
hexadecahydrorubroside D (9)	no change	>0.5		inactive	inactive
aurantoside A (10)	no change	>0.5		11.3	18.0
auroantoside B (11)	no change	>0.5		11.8	17.2

^a Morphological change at 0.1 μg/mL after 24 h. ^b Inhibitory zone (mm) at 2 μg/disk (8 mm).

Rubroside D (4). Red amorphous solid. $[\alpha]_D^{24}$ -1024° (*c* 0.001, MeOH); UV (MeOH) λ_{\max} 251 (ϵ 16 400), 432 (109 100) nm, UV (0.01 N HCl in MeOH) λ_{\max} 359 (23 600), 480 (101 800) nm, UV (0.01 N NaOH in MeOH) λ_{\max} 251 (20 000), 432 (123 600), 453 (112 700) nm; IR (film) 3360 (br), 3190, 2960, 2920, 1660, 1610, 1570, 1520, 1440, 1400, 1135, 1050 (br), 1000, 950, 765, 750 cm^{-1} ; HRFABMS (matrix: glycerol) *m/z* 937.2883 (M - H)⁻ (C₄₄H₅₆³⁵Cl₂N₂O₁₆ Δ -3.7 mmu); ¹H and ¹³C NMR data, see Table 1.

Rubroside E (5). Red amorphous solid. $[\alpha]_D^{24}$ -1424° (*c* 0.001, MeOH); UV (MeOH) λ_{\max} 243 (ϵ 17 000), 450 (61 700) nm; HRFABMS (matrix: glycerol) *m/z* 932.2304 (M - H)⁻ (C₄₁H₅₁³⁵Cl₃N₂O₁₆ Δ 0.0 mmu); ¹H and ¹³C NMR data, see Tables 3 and 4.

Rubroside F (6). Red amorphous solid. $[\alpha]_D^{24}$ -490° (*c* 0.001, MeOH); UV (MeOH) λ_{\max} 250 (ϵ 9100), 425 (80 000) nm, UV (0.01 N HCl in MeOH) λ_{\max} 348 (14 500), 468 (70 900) nm, UV (0.01 N NaOH in MeOH) λ_{\max} 250 (10 900), 425 (83 600), 450 (76 400) nm; IR (film) 3350 (br), 3180, 2910, 2840, 1660, 1610, 1575, 1550, 1520, 1440, 1400, 1135, 1070, 1040, 1000, 950, 750 cm^{-1} ; HRFABMS (matrix: glycerol) *m/z* 945.2413 (M - H)⁻ (C₄₂H₅₃³⁵Cl₃N₂O₁₆ Δ +3.0 mmu); ¹H and ¹³C NMR data, see Tables 3 and 4.

Rubroside G (7). Red amorphous solid. $[\alpha]_D^{24}$ -1212° (*c* 0.001, MeOH); UV (MeOH) λ_{\max} 248 (ϵ 32 400), 435 (154 400), 460 (175 500) nm; HRFABMS (matrix: glycerol) *m/z* 676.1985 (M - H)⁻ (C₃₃H₃₈³⁵Cl₂N₂O₉ Δ +3.1 mmu); ¹H and ¹³C NMR data, see Tables 2 and 4.

Rubroside H (8). Red amorphous solid. $[\alpha]_D^{24}$ -1308° (*c* 0.001, MeOH); UV (MeOH) λ_{\max} 245 (ϵ 13 700), 440 (44 700) nm; HRFABMS (matrix: glycerol) *m/z* 684.1372 (M - H)⁻ (C₃₁H₃₅³⁵Cl₃N₂O₉ Δ -3.6 mmu); ¹H and ¹³C NMR data, see Tables 3 and 4.

Hexadecahydrorubroside D (9). Colorless oil. $[\alpha]_D^{24}$ $+920^\circ$ (*c* 0.001, MeOH); UV (MeOH) λ_{\max} 243 (ϵ 20 300), 280 (20 300) nm; HRFABMS (matrix: glycerol) *m/z* 919.4500 (M - H)⁻ (C₄₄H₇₂³⁵Cl₂N₂O₁₆ Δ -7.0 mmu); ¹H NMR (C₅D₅N at 318 K) δ 4.47 (1H, m, H-25), 3.98 (1H, m, H-27), 3.75 (1H, dt, *J* = 3.7, 6.5 Hz, H-24), 3.41 (1H, br, H-5 β), 3.40 (2H, m, H-8), 3.30 (1H, br, H-5 α), 2.58 (1H, ddd, *J* = 7.3, 7.3, 14.7, H-26 β), 1.87 (1H, m, H-26 α), 1.85 (2H, m, H-23), 1.75 (2H, m, H-9), 1.44 (4H, m, H-10 and H-22), 1.34 (1H, d, *J* = 6.4, H-28), 1.23 (22H, brs, H-11 to H-21).

Methanolysis and Chiral GC Analysis of Rubrosides D (4) and F (6). Rubroside D (1.5 mg) in 10% HCl-MeOH (1.0 mL) was heated at 100 °C for 2 h. After evaporation of the solvent, the residue was chromatographed on ODS with H₂O and MeOH. The H₂O fraction was evaporated and reacted with trifluoroacetic anhydride (0.2 mL) in CH₂Cl₂ (0.2 mL) at 100 °C for 5 min. The reaction mixture was dried in a stream of N₂ and redissolved in CH₂Cl₂ (0.1 mL), and a 2 μL portion was subjected to GC analysis on a Chirasil-L-Val capillary column (25 m × 0.25 mm, i.d.): detection, FID; initial temperature 50 °C for 6 min, final temperature 160 °C for 1 min, temperature raised at 4 °C min⁻¹. Rubroside F was treated in the same way. Retention times: standard L-Xyl (16.785, 20.283 min), D-Xyl (16.427, 19.963 min), L-Ara (17.365, 20.325 min), D-Ara (17.385, 20.740 min); products from ru-

broside D, 15.833, 17.112, 19.025, and 20.545 min; products from rubroside F, 15.650, 16.795, 19.385, and 20.420 min. Because the retention times fluctuated, identity of the peaks was examined by co-injection with the standards. Absolute configuration of Xyl and Ara from 4 and 6 were both assigned as D.

Lemieux Oxidation, Acid Hydrolysis, and Chiral GC Analysis of Rubrosides D (4) and F (6). To a solution of rubroside D (ca. 1.0 mg) in H₂O (0.1 mL) were added KMnO₄ (0.25 mL of 10 mg/mL solution in H₂O) and NaIO₄ (0.3 mL of 10 mg/mL solution in H₂O), and the mixture was stirred at room temperature for 10 min. The reaction mixture was centrifuged for 10 min and filtered. The supernatant was evaporated to afford a residue which was dissolved in 6 N HCl (1.0 mL), and the mixture was heated at 105 °C for 2 h. After evaporation of the solvent, the residue was chromatographed on ODS with H₂O and MeOH. The H₂O fraction was dissolved in 10% HCl in MeOH (0.5 mL) and heated at 100 °C for 2 h. After removal of the solvent in a stream of N₂, CH₂Cl₂ (0.2 mL) and trifluoroacetic anhydride (0.2 mL) were added to the residue, and the mixture heated at 100 °C for 5 min. The solvents were removed in a stream of N₂, and the residue was redissolved in CH₂Cl₂ (0.1 mL). A 2 μL portion was subjected to GC analysis on a Chirasil-L-Val capillary column (25 m × 0.25 mm, i.d.): detection, FID; initial temperature 80 °C for 5 min, final temperature 200 °C for 10 min, temperature raised at 4 °C min⁻¹. Rubroside F was treated in the same way. Retention times: standard L-Asp (12.600 min), D-Asp (12.940 min); product from rubroside D (12.805 min); product from rubroside F (12.805 min). Because the retention times fluctuated, identity of the peaks was examined by co-injection with the standards. Absolute stereochemistry of Asp from 4 and 6 were both assigned as L.

Acid Methanolysis of Rubroside D. Rubroside D (8.0 mg, 8.5 × 10⁻³ mmol) in 10% HCl/MeOH (1.0 mL) was heated at 90 °C for 1 h. After evaporation of the solvent in a stream of nitrogen, the residue was purified by flash chromatography on ODS with H₂O, 10% MeOH, and 20% MeOH. The 10% MeOH eluate furnished sugar III (0.8 mg, yield 58%): ¹H NMR (CDCl₃) δ 1.31 (3H, d, *J* = 6.4 Hz, H-5), 3.37 (3H, s, 2-OMe), 3.40 (3H, s, 1-OMe), 3.63 (1H, d, *J* = 2.8, H-2), 4.05 (1H, dq, *J* = 6.7, 4.6, H-4), 4.88 (1H, brs, H-1), 3.70 (1H, dd, *J* = 3.1, 4.3, H-3).

(S)-(-)-MTPA Ester of Sugar III. To a stirred solution of sugar III (0.4 mg, 4.3 × 10⁻³ mmol) in dry pyridine (200 μL) was added (*R*)-(-)-MTPACl (7 μL), and the mixture was stirred at room temperature. After 1 h, additional (*R*)-(-)-MTPACl (7 μL) was added, and the mixture was stirred for 2 h at room temperature. The reaction mixture was purified by column chromatography on silica gel (hexane/EtOAc, 9:1) to furnish (*S*)-(-)-MTPA ester: ¹H NMR (CDCl₃) δ 7.686 (2H, m, Ph), 7.508 (3H, m, Ph), 5.238 (1H, dd, *J* = 4.6, 6.4 Hz, H-3), 4.875 (1H, d, *J* = 4.3, H-1), 4.040 (1H, dq, *J* = 4.6, 6.1, H-4), 3.907 (1H, dd, *J* = 4.3, 6.4, H-2), 3.541 (3H, s, OMe), 3.428 (3H, s, 1-OMe), 3.250 (3H, s, 2-OMe), 1.495 (3H, d, *J* = 6.1, H-5).

(R)-(+)-MTPA Ester of Sugar III. Sugar III (0.4 mg, 4.3 × 10⁻³ mmol) in dry pyridine (200 μL) and (*S*)-(+)-MTPACl (7

